Trajectory studies of unimolecular reactions of Si2H4 and SiH2 on a global potential surface fitted to a b i n i t i o and experimental data

Paras M. Agrawal, Donald L. Thompson, and Lionel M. Raff

Citation: The Journal of Chemical Physics **89**, 741 (1988); doi: 10.1063/1.455197
View online: http://dx.doi.org/10.1063/1.455197
View Table of Contents: http://scitation.aip.org/content/aip/journal/jcp/89/2?ver=pdfcov
Published by the AIP Publishing

Trajectory studies of unimolecular reactions of Si_2H_4 and SiH_2 on a global potential surface fitted to *ab initio* and experimental data

Paras M. Agrawal,[a] Donald L. Thompson, and Lionel M. Raff
Department of Chemistry, Oklahoma State University, Stillwater, Oklahoma 74078

(Received 11 February 1988; accepted 8 April 1988)

The unimolecular decomposition dynamics of Si_2H_4 have been investigated using classical trajectory methods on a global potential-energy surface fitted to the results of *ab initio* calculations and the available experimental data. The required phase-space averages are computed using Metropolis sampling techniques. It is found that unless the parameters of the Markov walk are adjusted for each different type of atom present, extremely long Markov walks are required to adequately cover the phase space of the system. Microcanonical rate coefficients for the decomposition of Si_2H_4 into all open channels are reported at energies in the range $5.0 < E < 9.0$ eV. The most important dissociation channel over this energy range is three-center elimination of molecular hydrogen leading to $H_2Si{=}Si$. At energies below 7.0 eV, the other channels are, in order of importance, Si–Si bond rupture, four-center H_2 elimination, and simple Si–H bond rupture. At or above 8.0 eV, four-center H_2 elimination replaces Si–Si bond rupture as the second most important decomposition channel. The energy dependence of the rate coefficients is well described by an RRK expression. Three-center H_2 elimination involves a simultaneous rupture of both Si–H bonds whereas the four-center elimination is found to proceed by a hydrogen atom transfer process followed by H_2 elimination. Except for a small propensity to form H_2 with excess rotational energy, the energy partitioning among the products is nearly statistical. A comparison study of the decomposition of Si_2H_4 complexes formed by the recombination of two SiH_2 molecules shows that the rates for both three- and four-center H_2 elimination are in agreement with those computed using a statistical distribution of the same internal energy. The rate for Si–Si bond rupture, however, is significantly larger for Si_2H_4 complexes formed by SiH_2 recombination than for Si_2H_4 molecules with the same internal energy randomly distributed. The decomposition dynamics of SiH_2 on the global surface are also reported.

I. INTRODUCTION

We have recently reported[1] (hereafter referred to as paper I) an empirical potential-energy surface for the Si_2H_4 system which is fitted to the available experimental data reported by Berkowitz *et al.*[2] and to the results of *ab initio* calculations by Ho *et al.*,[3] Peyerimhoff and Buenker,[4] Gordon *et al.*,[5] and Binkley[6] for heats of reaction and equilibrium structures of Si_2H_4, $H_2Si{=}SiH$, $H_2Si{=}Si$, $HSi{=}SiH$, SiH_2, and Si_2, and fundamental vibrational frequencies for Si_2H_4, $H_2Si{=}SiH$, $H_2Si{=}Si$, and SiH_2. The availability of such a global surface greatly facilitates the investigation of various gas-phase reactions of importance in the chemical vapor deposition (CVD) of silicon from silane.

Silylene is the primary product of silane unimolecular dissociation. Disilene, Si_2H_4, can be formed either by recombination of two SiH_2 molecules or by the dissociation of disilane, Si_2H_6, formed by the condensation of SiH_4 with SiH_2. In paper I, we have employed the Si_2H_4 global potential-energy surface to compute the recombination rates and cross sections for the formation of disilene via SiH_2 recombination.

Once formed, Si_2H_4 may undergo a series of unimolecular reactions eventually leading to the formation of Si_2. The initial steps in this process are

$$Si_2H_4 \rightarrow SiH_2 + SiH_2, \quad \text{(R1)}$$

$$Si_2H_4 \rightarrow H_2Si{=}Si + H_2, \quad \text{(R2)}$$

$$Si_2H_4 \rightarrow HSi{=}SiH + H_2, \quad \text{(R3)}$$

and

$$Si_2H_4 \rightarrow H_2Si{=}SiH + H. \quad \text{(R4)}$$

Reaction (R1) is the reverse of the silylene recombination process studied in paper I. Reactions (R2) and (R3) are three- and four-center molecular hydrogen elimination channels, and reaction (R4) is the simple two-center Si–H bond rupture process.

Subsequent to these reactions, the products may undergo further dissociation to yield the Si_2 dimer which has been found to make a significant contribution to the total silicon chemical vapor deposition rate.[7] That is, we may expect to observe

$$H_2Si{=}Si \rightarrow Si_2 + H_2 \quad \text{(R5)}$$

and

$$HSi{=}SiH \rightarrow Si_2 + H_2. \quad \text{(R6)}$$

Silylene itself dissociates by both two- and three-center processes:

[a] On leave from Vikram University, Ujjain, MP, India.

 0021-9606/88/140741-10$02.10

$$SiH_2 \rightarrow Si + H_2 \quad \text{(R7)}$$

and

$$SiH_2 \rightarrow SiH + H. \quad \text{(R8)}$$

Rate coefficients for these two reactions have been computed by NoorBatcha *et al.*[8] using the semiempirical valence bond potential-energy surface developed by Viswanathan *et al.*[9] This surface is fitted to the Si–H bond energies reported by Walch[10] and by Doncaster and Walch.[11] However, more accurate recent experimental data reported by Berkowitz *et al.*[2] and the *ab initio* calculations reported by Ho *et al.*[3] show that the SiH_2 heat of formation is significantly higher than that indicated by the previous studies and that the Si–H bond energies are much lower. As a result, the endothermicities for reactions (R7) and (R8) given by the fitted valence–bond surface,[8] 2.418 and 3.825 eV, respectively, are too large and the corresponding rates obtained for reactions (R7) and (R8) using this surface are too small.

The above errors may be corrected by reexamination of reactions (R7) and (R8) using the Si_2H_4 global potential-energy surface.[1] This surface yields endothermicities of 1.486 and 3.278 eV for reactions (R7) and (R8), respectively, in excellent agreement with the *ab initio* results[3] and with the experimental data.[2]

In this paper, we investigate the dynamics of reactions (R1), (R2), (R3), (R4), (R7), and (R8). Rate coefficients, product energy distributions, and reaction mechanisms are determined for each reaction using classical trajectory methods. All reactions are studied for conditions corresponding to initially complete randomization of the internal energy obtained by using Metropolis sampling methods. In addition, we also report results for Si_2H_4 decomposition in which the initial states are taken from the results of paper I in which Si_2H_4 is formed via recombination of two SiH_2 molecules. Section II describes the computational methods with particular emphasis on the problems associated with the Metropolis sampling procedures. The results are given and discussed in Sec. III. Section IV summarizes our findings.

II. METHODS

The unimolecular reaction dynamics of reactions (R1), (R2), (R3), (R4), (R7), and (R8) have been investigated using standard classical trajectory methods[12] on the global potential-energy surface described in I. Microcanonical rate coefficients have been computed at several internal energies from the results of batches of 200 trajectories at each energy. The initial state sampling has been effected using microcanonical Metropolis sampling procedures.[12,15,16] Hamilton's equations are integrated using a Runge–Kutta algorithm with a fixed stepsize of 1.019×10^{-16} s. In most of the calculations, trajectories were integrated until dissociation occurred or up to a maximum of 20 000 time steps for reaction involving Si_2H_4 or 5000 time steps for the dissociation of SiH_2. However, in one set of calculations for Si_2H_4 with internal energies less than 5.0 eV, the maximum integration time was increased to 40 000 integration steps.

Microcanonical rate coefficients have been computed by assuming that all reactions are described by a first-order rate law. This gives

$$K_T(E) = \sum_i k_i(E), \quad (1)$$

$$N = N_0 \exp[-K_T(E)t], \quad (2)$$

and

$$k_i(E)/k_j(E) = N_i(t)/N_j(t), \quad (3)$$

where the $k_i(E)$ are microcanonical rate coefficients for decomposition into channel i at internal energy E. The sum in Eq. (1) runs over all open channels. N is the number of trajectories that have not dissociated at time t and N_0 is the total number of trajectories studied. $N_i(t)$ and $N_j(t)$ are the number of reactions into channels i and j, respectively, at time t.

Each of the above procedures, except for the Metropolis sampling, is straightforward. The initial-state selection, however, presents some problems. These problems arise because of the multidimensional nature of the Si_2H_4 system which makes it difficult for the Markov walk to adequately cover the entire phase space of the system.

In the usual procedure, Si_2H_4 is placed in its equilibrium configuration and the desired total internal energy E is inserted as kinetic energy partitioned equally among all of the momentum components. For SiH_2, the initial energy is partitioned such that both hydrogen atoms have equal energy with the total linear momentum being zero. A trajectory is then computed to allow the exchange of kinetic and potential energy in the molecule. This trajectory is run until a configuration is attained for which the kinetic and potential energies are approximately equal. At this point, 20 000 warmup moves are made in the microcanonical Markov walk through the system phase space. In this context, we define one move to be a one-step walk in each of the 36 dimensions of the Si_2H_4 phase space.

In each Markov step, the new Cartesian momenta and coordinates at the $(n+1)$th move are obtained from those at the nth move using

$$q_i^{(n+1)} = q_i^{(n)} + (\xi - 0.5)dq_i \quad (4)$$

and

$$p_i^{(n+1)} = p_i^{(n)} + (\xi - 0.5)dp_i\,. \quad (5)$$

Here, $\xi = \xi(i,n)$ is a random number with uniform distribution over the range [0,1]. The new configuration is rejected if the new phase space point lies too far off the energy shell. That is, we require that

$$|E^{(n+1)} - E^{(n)}| < dE. \quad (6)$$

The move is also rejected if a newly selected random number satisfies the inequality

$$\xi > P^{(n+1)}/P^{(n)}, \quad (7)$$

where $P = P(q,p)$ is, in principle, the Dirac delta function, $\delta[E - H(q,p)]$, with H being the system Hamiltonian. Such a choice, however, is not practical. The delta function is therefore replaced with its prelimit form:

$$P(q,p) = S/\{S^2 + [E - H(q,p)]^2\}^{1/2}. \quad (8)$$

In addition to these restrictions, a move is also rejected if two hydrogen atoms come closer than 1.30 Å or if any bond length exceeds 30% of the equilibrium bond distance.

It has been suggested[15,16] that coverage of phase space is most efficiently achieved by using walk parameters that yield an acceptance-to-rejection ratio near unity. However, since this ratio depends upon four parameters, S, dE, dq_i, and dp_i, some criterion other than this ratio is needed to select the optimum set of parameters. In this connection, it is also necessary to have an estimate of the number of moves required to cover a reasonable portion of the available phase space for a given set of walk parameters. Convergence of the final trajectory results is not a sufficient criterion for testing this coverage because of the possibility of convergence in a small subset of phase space. That is, if L moves are actually required to adequately cover phase space, it is still possible for the results of two trajectory calculations with sets of $L/1000$ and $L/500$ moves, respectively, to appear to converge since both calculations would be covering almost the same small portion of the phase space and therefore give the same "converged" results.

For a one-dimensional random walk with stepsize dw, the probability of being at a distance w at the nth move can be shown to be[17]

$$p_n(w) = n!/[(n/2 + w/2)!(n/2 - w/2)!2^n]. \quad (9)$$

For large n, we have

$$\lim_{n\to\infty} p_n(w) \to [2/\pi n]^{1/2}\exp\{-w^2/2n\}. \quad (10)$$

The probability $p(w,N)$ that the system will have been at the distance w in N moves is therefore

$$p(w,N) = 1 - \prod_{n=1}^{N} [1 - p_n(w)]. \quad (11)$$

Equation (11) indicates that a large number of moves will be required to cover the phase space of molecular systems. As an example, consider a Markov walk for a simple Si_2 diatomic molecule which is given 1.0 eV initial kinetic energy. For simplicity, assume the vibrational motion of this molecule may be treated as a one-dimensional harmonic oscillator with a force constant equal to that for the Si–Si interaction given in paper I. We now execute a Markov walk according to Eqs. (4)–(8) to determine the number of moves required to change the Si_2 vibrational phase by 180° starting from its equilibrium configuration. For the set of parameters, $S = 0.005$ eV, $dE = 0.1$ eV, $dq = 0.005$ Å, and $dp = 0.01$ momentum units, we find an acceptance/rejection ratio which is nearly unity and a requirement of 6.1 million moves. Very similar results are obtained using Eqs. (9)–(11). With $dp = 4dw = 0.01$ momentum units, we find that $p(w,N)$ approaches unity for $N = 2.6$ million moves for the same distance w. In the multidimensional phase space of Si_2H_4, the problem of adequate coverage becomes even more accute.

Equations (9)–(11) show that the rate of phase space coverage is significantly increased by increasing dw. For example, for coverage of the same distance w in momentum space, $p(w,N)$ tends to unity for $N = 0.77$, 0.38, 0.23, 0.16, and 0.11 million moves for $dp = 4dw = 0.02$, 0.03, 0.04, 0.05, and 0.06, respectively. Equations (4)–(8) also predict similar increases in the coverage rate with increases in the stepsize. It is found that 0.87 and 0.22 million moves are required for $dp = 0.03$ and 0.06, respectively, compared to 6.1 million moves required for $dp = 0.01$. The number of required moves depends upon the initial seed for the random number generator. The above numbers represent the minimum of three sets run for each case. The use of larger stepsizes, however, may significantly reduce the acceptance/rejection ratio. This problem may be reduced by the use of different stepsizes for different atoms in the system. Generally, larger momentum steps may be used for heavier atoms than for lighter atoms. Consequently, we have taken the momentum stepsize for silicon to be larger than that for hydrogen by a factor equal to the square root of the ratio of the two masses. For the coordinate step dq, the inverse criterion is used. The values of the Markov walk parameters used in the present calculations are given in Table I.

In addition to the convergence of the trajectory results, we have used the following criteria to test the adequacy of the phase space coverage achieved by the Markov walk. A random selection of a large number of phase space points over the complete phase space of the Si_2H_4 molecule must give

$$\langle T\rangle = \langle V\rangle, \quad (12)$$

$$\langle p_j\rangle_i = 0, \quad j = 1,2,3; \quad i = 1\text{–}6, \quad (13)$$

where $\langle\ \rangle$ denotes the average over all covered phase space points, T and V are the kinetic and potential energy, respectively, and p_j is the jth Cartesian momentum component for atom i. Similarly, we expect equality of the average kinetic energy of similar types of atoms:

$$\langle T\rangle_{Si(1)} = \langle T\rangle_{Si(2)} \quad (14)$$

and

$$\langle T\rangle_{H(1)} = \langle T\rangle_{H(2)} = \langle T\rangle_{H(3)} = \langle T\rangle_{H(4)}, \quad (15)$$

where the numbers in parentheses denote atom numbers.

In practice, we execute 20 000 warmup moves as described above and then select phase space points separated by 300 moves. At each internal energy, 2000 such points are selected in this manner. The starting conditions for each of the trajectories are made by a random selection of 200 of these 2000 points. In each case, the total internal energy lies in the range $E - dE < E < E + dE$. All momenta are therefore scaled before integration so that the total energy becomes exactly E. The usual recounting procedures are used throughout the walk.

TABLE I. Parameter values for the microcanonical Markov walk.

Parameter	Value
S	0.02 eV
dE	0.20 eV
dq(Si)	0.002 5 Å
dq(Si)	0.060 mu[a]
dq(H)	0.013 25 Å
dq(H)	0.011 32 mu[a]

[a] 1 mu = 1 amu Å/tu, where 1 tu = 1.019×10^{-14} s.

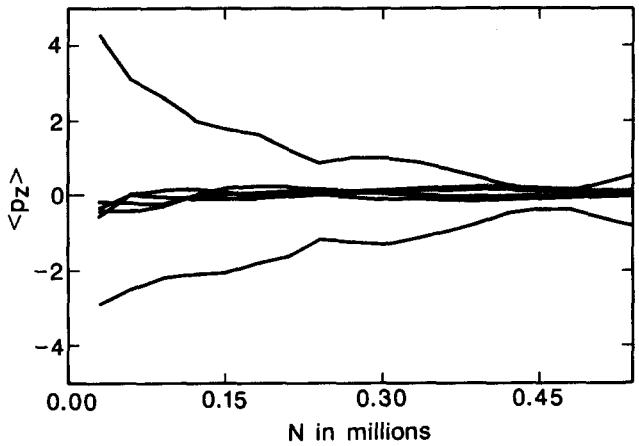

FIG. 1. $\langle p_z \rangle_i$ ($i = 1$–6) in momentum units as a function of the number of moves N in phase space. The curves with large amplitude correspond to the two silicon atoms and the remaining four curves are for the hydrogen atoms of Si_2H_4. $E = 7.0$ eV.

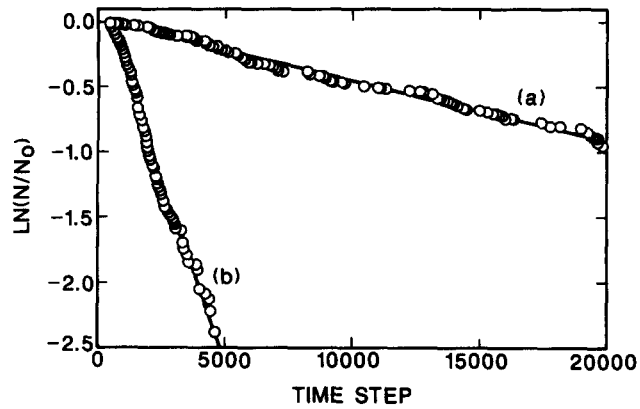

FIG. 3. $\ln[N/N_0]$ vs time step for the unimolecular dissociation of Si_2H_4 at internal energy (a) 6.0 eV, (b) 9.0 eV. The circles are trajectory results and the straight lines are the least-squares fits. One time step is 1.019×10^{-16} s.

We find that the phase space points generated in the Markov walk satisfy Eqs. (12), (14), and (15) within 25%. Figure 1 shows the variation of $\langle p_j \rangle_i$ as a function of the number of Markov moves N over which the average has been taken. The averaging is clearly adequate for the hydrogen atoms, but much less so for the two silicon atoms. Figure 2 shows p_z for one of the silicon atoms as a function of N. The variation of this momentum over both positive and negative values indicates that the random walk is covering most of the available phase space even though it is not sufficiently long to guarantee that Eq. (13) holds for the silicon atoms.

III. RESULTS AND DISCUSSION

A. Rate coefficients for Si_2H_4

Microcanonical dissociation rate coefficients for reactions (R1), (R2), (R3), and (R4) have been computed at Si_2H_4 internal energies of 5.0, 6.0, 7.0, 8.0, and 9.0 eV by using Eqs. (1)–(3) to analyze the trajectory data. With the exception of the $E = 5.0$ eV case, decomposition has been followed for at least one half-life. The actual number of dissociating trajectories observed are 29, 122, 183, 199, and 200 out of 200 at 5.0, 6.0, 7.0, 8.0, and 9.0 eV, respectively. First-order decay plots for the results at 6.0 and 9.0 eV are shown in Fig. 3. The excellent linearity of the results confirm the concurrent first-order nature of reactions (R1), (R2), (R3), and (R4). The slope of the decay plots yield the corresponding $K_T(E)$ values and the product ratios give the individual rate coefficients. These results are given in Table II.

RRK theory suggests that the microcanonical rate coefficient is given by

$$k(E) = f[(E - E_0)/E]^{s-1}, \tag{16}$$

where E_0 and s are the critical energy for reaction and the number of effective internal degrees of freedom participating in the reaction. The critical energy for reaction (R1) is taken to be the reaction endothermicity, 3.49 eV, since there is no barrier to the backreaction on the Si_2H_4 global potential surface.

Figure 4 shows the reaction profile for the three-center molecular hydrogen elimination channel (R2) along a symmetric C_{2v} dissociation pathway described in paper I for the analogous reaction (R7). This profile is obtained by varying the angle made by the hydrogen displacement vector with the C_{2v} axis at each step to find the minimum-energy displacement pathway. Simultaneously, the backside $H_2Si{=}Si$ moiety is relaxed to its equilibrium configuration at each

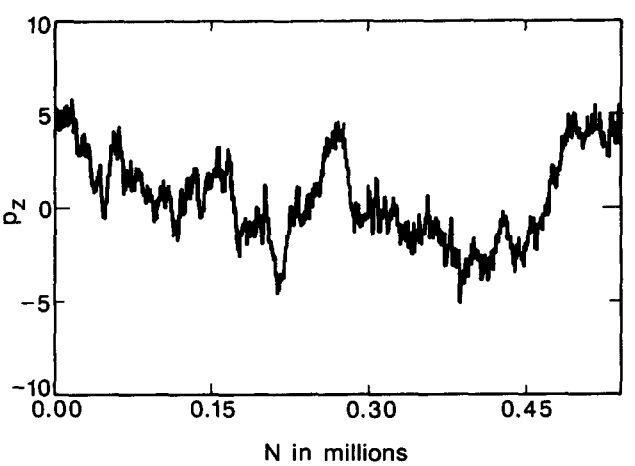

FIG. 2. p_z in momentum units for a silicon atom of Si_2H_4 as a function of the number of moves N in phase space. $E = 7.0$ eV.

TABLE II. Microcanonical rate coefficients for different Si_2H_4 dissociation channels.[a]

E (eV)	$k_1(E)$	$k_2(E)$	$k_3(E)$	$k_4(E)$
5.0	0.0060	0.073	0.0015	0.0[b]
6.0	0.077	0.35	0.045	0.0[b]
7.0	0.24	0.91	0.18	0.063
8.0	0.46	1.81	0.47	0.22
9.0	1.02	3.20	1.15	0.23

[a]Rate coefficients are given in units of s^{-1} and are scaled by a factor of 10^{-12}.

[b]Zero entries mean no trajectories were observed to dissociate into this channel.

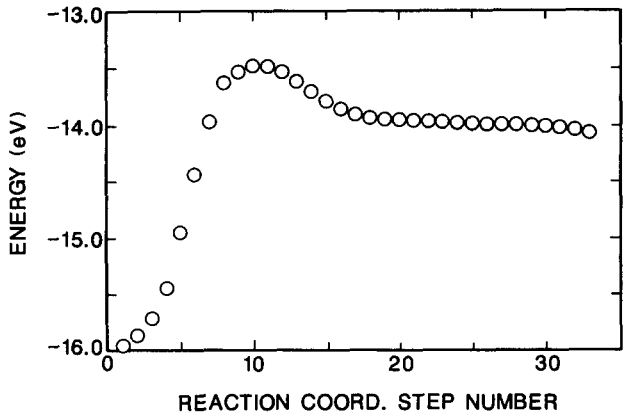

FIG. 4. Reaction profile for the three-center molecular elimination reaction from Si_2H_4. Each step corresponds to a C_{2v} symmetric displacement of each Si–H bond by dx at an angle with the C_{2v} axis that corresponds to the minimum barrier path. $dx = 0.1$ Å except near the peak at which $dx = 0.05$ Å. The backside H_2Si=Si moiety is allowed to relax at each step.

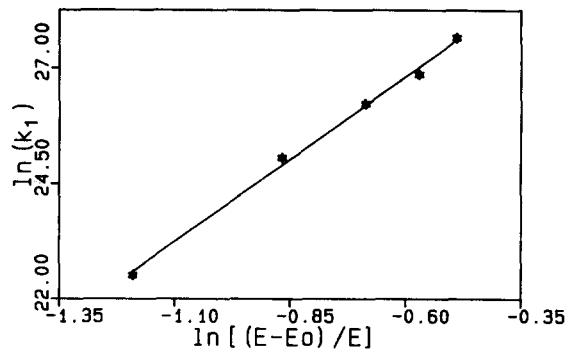

FIG. 5. RRK plot for the rate coefficient for reaction (R1). The rate coefficient $k_1(E)$ is given in s^{-1}. Stars denote the trajectory results. The line is the least-squares fit for $E_0 = 3.49$ eV.

displacement step using trajectory methods. These calculations show that the potential barrier for reaction (R2) is 2.50 eV which we take to be the critical energy. The results also show that the backreaction corresponding to H_2 insertion into H_2Si=Si has a barrier of 0.68 eV on the present global potential surface.

For the four-center H_2 displacement reaction (R3) the upper limit of the barrier height calculated in paper I is 5.0 eV. However, in the present trajectory calculations at a total internal energy of 5.0 eV, we found one trajectory leading to reaction (R3) such that the maximum potential energy of the system relative to its equilibrium energy was 4.54 eV. Consequently, the barrier for (R3) must be equal to or less than this value. The endothermicity of reaction (R3), 3.67 eV, provides a lower limit to the potential barrier. We therefore expect the critical energy to lie in the range $3.67 \text{ eV} < E_0 < 4.54$ eV. The results for several values in this range have been investigated.

The endothermicity for reaction (R4) is 4.37 eV which we expect to correspond to the potential barrier since the backreaction probably has no barrier. Since Table II shows $k_3(E) > k_4(E)$ for all E, we expect to have $(E_0)_4 > (E_0)_3$. This suggests that the actual potential barrier for reaction (R3) does not lie toward the upper end of the above range.

Table III shows the least-squares fit of the data in Table II to Eq. (16). For reaction (R3), the results are given for several choices of E_0 spanning the range $3.67 \text{ eV} < E_0 < 4.54$ eV. In all cases, the RRK expression provides a good fit to the trajectory data. Figures 5–7 show the resulting RRK plots for reactions (R1), (R2), and (R3), respectively. For reactions (R1) and (R3), the results yield s values in the range 5.45–8.42. These results are not particularly surprising since it is generally found that the number of effective vibrational degrees of freedom is about half the total number. In contrast, we find $s = 11.2$ for reaction (R2) which suggests that virtually all of the 12 Si_2H_4 vibrational modes participate in the three-center H_2 elimination reaction.

In all of the above calculations, the total Si_2H_4 internal energy is randomly distributed by the Metropolis sampling procedures described in Sec. II. Consequently, the results in Table II correspond to the classical RRK rates. In paper I, we have reported rate coefficients for the recombination reaction

$$SiH_2 + SiH_2 \rightarrow Si_2H_4. \qquad \text{(R9)}$$

In these calculations, 150 trajectories were integrated with the relative translational energies thermally averaged at 800 K. A total of 62 Si_2H_4 complexes were formed with an average internal energy of 4.48 eV. It has been suggested[7(a)] that the decomposition of these complexes is the major pathway leading to the formation of Si_2 dimers which have been shown to be responsible for over 50% of the silicon deposition rate in silicon CVD experiments provided the carrier gas is helium. It is possible that the decomposition of Si_2H_4 complexes formed in reaction (R9) will follow RRK/RRKM kinetics. However, since the initial energy

TABLE III. RRK parameters for reactions (R1), (R2), and (R3).[a]

Parameter	(R1)	(R2)	(R3)				
E_0	3.49	2.50	3.8	4.0	4.2	4.4	4.54
s	8.15	11.2	8.42	6.38	6.40	5.47	5.45
f	0.32	0.85	0.64	0.44	0.31	0.18	0.22

[a] E_0 is given in eV. f is given in $s^{-1} \times 10^{14}$.

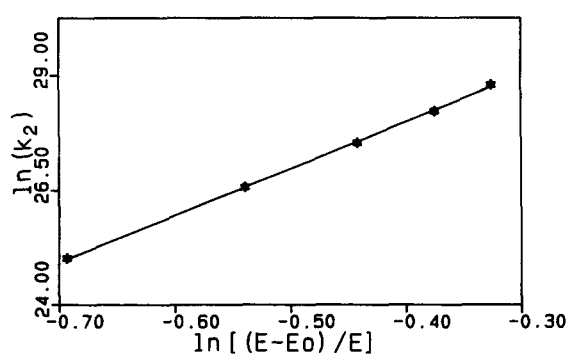

FIG. 6. Same as Fig. 5 but for reaction (R2) with $E_0 = 2.50$ eV.

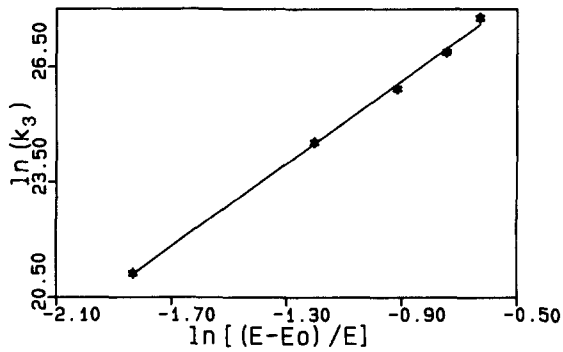

FIG. 7. Same as Fig. 5 but for reaction (R3) with $E_0 = 4.20$ eV.

distribution in these complexes is not random, this is not necessarily the case.

To investigate this point, we have followed the evolution of the Si_2H_4 complexes formed in paper I through 4.076×10^{-12} s (40 000 time steps). We find that in this period the number of complexes dissociating via channels (R1), (R2), and (R3) are 3, 5, and 1, respectively. Extrapolation of the microcanonical rate coefficients for reactions (R1), (R2), and (R3) using Eq. (16) and the data in Table II indicates that if reaction of the Si_2H_4 complexes corresponds to that expected for a random initial distribution of internal energy, there should be 5 decompositions into channel (R2) out of 62 complexes within 4.076×10^{-12} s. In contrast, the number of reactions into channels (R1) and (R3) would both be less than 1. Equation (16) therefore correctly predicts the observed results, within the expected statistical error, for reactions (R2) and (R3), but not for (R1). The decomposition of Si_2H_4 complexes formed in reaction (R9) via Si–Si bond rupture is significantly faster than would be expected for a random distribution of the internal energy.

The large rate of dissociation into channel (R1) is qualitatively consistent with the fact that the 3.49 eV of energy liberated during reaction (R9) is primarily partitioned into the Si–Si stretching modes. This results in an initial rate for decomposition into channel (R1) that is much larger than the rate computed for a random distribution of 3.49 eV of energy throughout the molecule. In contrast, molecular hydrogen elimination via reactions (R2) or (R3) requires initial energy transfer out of the Si–Si stretching modes prior to reaction. As a result, the internal energy distribution in molecules undergoing reactions (R2) and (R3) is more nearly random and the rate coefficients are nearly equal to the RRK rates.

TABLE IV. Distribution of energy in the dissociation products of Si_2H_4. $\langle F_T \rangle$, $\langle F_R \rangle$, and $\langle F_V \rangle$ denote average fractions of energy partitioned into translation, rotation, and vibration, respectively.

E (eV)	$\langle F_T \rangle$	$\langle F_R \rangle$	$\langle F_V \rangle$
5.0	0.18	0.25	0.57
7.0	0.18	0.22	0.59

TABLE V. Distribution of energy among the products of different dissociation channels of SiH_4 at $E = 7.0$ eV. $\langle F_T \rangle$, $\langle F_R \rangle$, and $\langle F_V \rangle$ denote average fractions of energy partitioned into translation, rotation, and vibration, respectively.

Reaction	$\langle F_T \rangle$	$\langle F_R \rangle$	$\langle F_V \rangle$
(R1)	0.26	0.21	0.53
(R2)	0.16	0.24	0.60
(R3)	0.21	0.19	0.60

B. Product energy distributions

Table IV gives the distribution of translational, rotational, and vibrational energies in the dissociation products of Si_2H_4 at internal energies of 5.0 and 7.0 eV. Table V gives the same information for the products of different reaction channels at 7.0 eV. In both tables $\langle F_T \rangle$, $\langle F_R \rangle$, and $\langle F_V \rangle$ denote the average fractions of energy partitioned into translational, rotational, and vibrational motion of the products, respectively. The "rotational energy" has been computed from

$$E_{\rm rot} = L^2/2I, \tag{17}$$

where L is the angular momentum about the center of mass and I is the moment of inertia about an axis passing through the center of mass in the direction of the angular momemtum vector. The vibrational energy has been obtained by difference between the total internal energy and the rotational energy. In every case, most of the available energy is partitioned into vibrational modes. This type of result is typical of the data obtained in many MPD experiments. For example, Holmes and Setser[18] have measured the fraction of the total energy remaining in the organic product upon four-center dissociation of HCl from several substituted cyclobutanes and find that an average of 60% of the total energy remains in vibrational modes of the olefin after dissociation. Similar results have been reported by Clough, Polanyi, and Taguchi[19] and by Berry and Pimentel[20] for HF elimination from 1,1,1-trifluoroethane.

The product energy distributions are very nearly statistical. A completely statistical distribution would place 20% of the energy into translational modes. The values in Table V range between 0.16–0.26. Table VI gives the energy distributions among different products for reactions (R2) and (R3)

TABLE VI. Distribution of energy among different products of different dissociation channels of Si_2H_4. $E = 7.0$ eV. Other notation is defined as in Table V.

	$\langle F_T \rangle$		$\langle F_R \rangle$		$\langle F_V \rangle$	
Reaction	Si_2H_2	H_2	Si_2H_2	H_2	Si_2H_2	H_2
(R2)	0.005	0.15	0.11	0.13	0.45	0.15
(R3)	0.007	0.20	0.11	0.09	0.47	0.13

at 7.0 eV. The ratio of Si_2H_2 to H_2 translational energy is, of course, determined solely by their respective masses. Since there are nine internal degrees of freedom in Si_2H_2 and only three in H_2, a completely statistical distribution would yield $[\langle F_R\rangle + \langle F_V\rangle]_{Si_2H_2}/[\langle F_R\rangle + \langle F_V\rangle]_{H_2} = 3.0$. The trajectory calculations give values of 2.0 and 2.6 for this ratio for reactions (R2) and (R3), respectively. Most of the difference between these values and the purely statistical result is due to extra energy partitioned into H_2 rotational motion. The dynamics of the dissociation process on the Si_2H_4 global potential surface do not correspond to a symmetric H_2 elimination pathway. The mechanism must frequently involve asymmetric dissociation which provides a torque and angular momemtum to the departing H_2 molecule.

C. Qualitative aspects of the dissociation mechanisms

The distance notation used in the following discussion is defined in Fig. 8. Figure 9 shows the time variation of various distances in a typical trajectory for reaction (R1). The variation of the Si–Si distance, curve (a), shows that dissociation occurs around 8000 time steps. The decrease in the Si–Si stretching frequency with increasing amplitude seen in this curve is due to the anharmonicity of the bond potential. Distance R_{10} is shown as a function of time in curve (b). This distance effectively measures the SiH_2 bending motion. The increased frequency of this motion after dissociation reflects the fact that the SiH_2 bending frequency for Si_2H_4 is less than the corresponding frequency for SiH_2. The loss of energy from the bending mode upon dissociation is obvious from the decreased amplitude. This mode is clearly active for dissociation via channel (R1). In contrast, the Si–H vibrational motion shown by curve (c) is hardly affected by the dissociation process. The Si–Si and Si–H stretching modes are only weakly coupled. Energy transfer between them consequently plays only a minor role in Si–Si bond rupture. Curve (d) shows the potential energy of the system relative

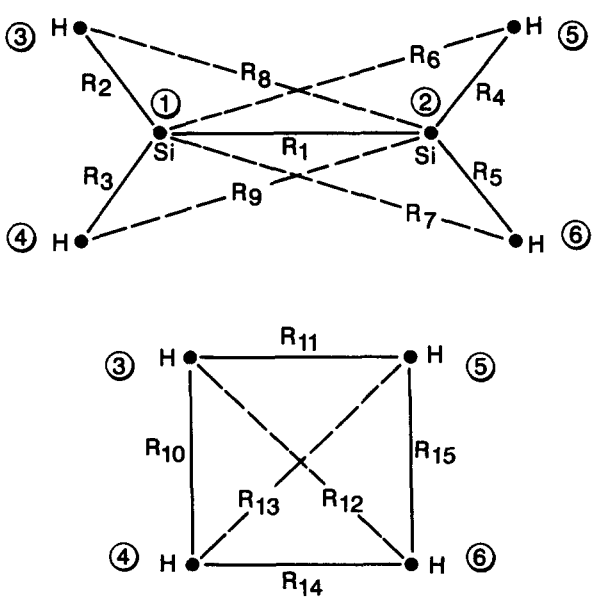

FIG. 8. Definition of interatomic distances. The atom number designations are circled.

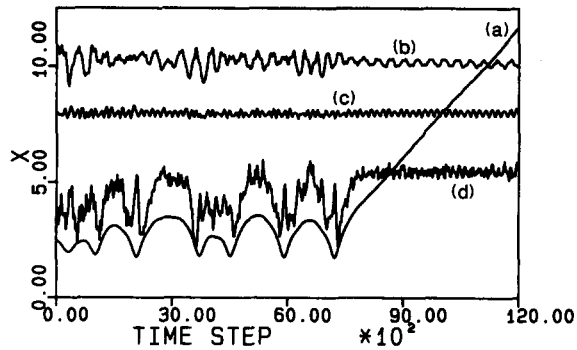

FIG. 9. Time variation of various dynamical quantities for Si_2H_4 for reaction (R1) with initial energy of 5.0 eV. Curve (a): $X = R_1$; curve (b): $X = R_{10} + 8.0$ Å; curve (c): $X = R_2 + 6.5$ Å; curve (d): $X = V_{eq} + 1.5$ eV, where V_{eq} is the potential energy relative to the equilibrium position of disilene. Distances are in Å and one time step is 1.019×10^{-16} s. Distance notation is as defined in Fig. 8.

to Si_2H_4 in its equilibrium configuration. Prior to dissociation, the oscillation of the potential energy mirrors the Si–Si vibration frequency. Subsequent to dissociation, the potential oscillates with a frequency characteristic of Si–H motion. The rapid equilibration of energy between the bend and stretch in SiH_2 may also be seen here. The rise in potential at the point of dissociation depicts the endothermicity of the reaction.

Figures 10 and 11 shows the mechanistic details for typical dissociations occurring via reaction (R2). Figure 10 shows (R2) to be a concerted three-center elimination rather than a "half-reaction" of $H + Si_2H_3$. The two Si–H distances are seen to increase simultaneously around 9300 time steps as molecular H_2 is formed. Figure 11 shows the variation of the Si–Si and the other Si–H distances during the same reaction. The lack of variation of the Si–H amplitudes during the reaction shows that these vibrational modes are not involved in the three-center elimination reaction. The Si–Si bond, however, is coupled and the flow of energy out of this stretching mode as the reaction occurs is obvious.

The details for four-center H_2 elimination, reaction (R3), are shown by Figs. 12–14. Figure 12 shows the Si–H distances for the dissociating hydrogen atoms along with the corresponding H–H distance. In this case, we see that the

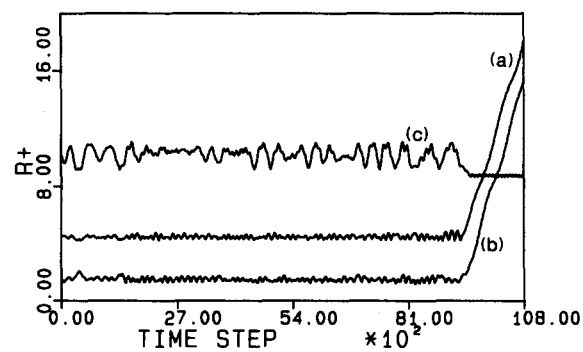

FIG. 10. Same as Fig. 9 but for a trajectory leading to reaction (R2). Curve (a): $R+ = R_2 + 3.0$ Å; curve (b): $R+ = R_3$; curve (c): $R+ = R_{10} + 8.0$ Å.

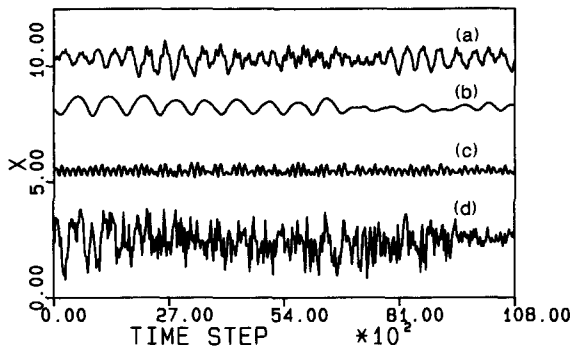

FIG. 11. Same as Fig. 10. Curve (a): $X = R_{15} + 8.0$ Å; curve (b): $X = R_1 + 6.0$ Å; curve (c): $X = R_4 + 4.0$ Å; curve (d): $X = V_{eq}$.

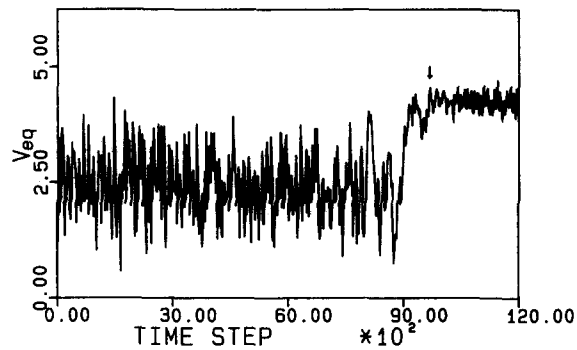

FIG. 13. Same as Fig. 12 but for the potential relative to the equilibrium structure of Si_2H_4.

mechanism involves a hydrogen transfer from one silicon atom to other. This is immediately followed by rupture of the second Si–H bond to form H_2. Simultaneous detachment of both hydrogen atoms is not observed in this process. Figure 13 shows the variation of the potential throughout the reaction. The potential rises sharply as H_2 elimination takes place, reaching a maximum value of 4.54 eV at time step 9700 (marked by the arrow in Fig. 13). These results show that the potential barrier height for reaction (R3) must be less than or equal to 4.54 eV. The contributions of the vibrational modes involving Si–Si and Si–H motion are shown in Fig. 14. Again it is clear that there is little or no coupling between the Si–H modes and the dissociation coordinate. The Si–Si stretch is, however, coupled to this coordinate as is the case for three-center dissociation.

D. Dissociation of SiH_2

We have reexamined the dissociation dynamics for SiH_2 on the present Si_2H_4 potential surface. Reactions (R7) and (R8) have lower potential barriers on this surface than on the valence bond surface[8] employed in our previous studies of this system.[8] Consequently, we find that the microcanonical rate coefficients are larger than those we previously reported.[8] Rate coefficients at total energies of 3.0, 3.5, 4.0, and 4.5 eV have been computed using batches of 200 trajectories at each energy. The results are given in Table VII. Table VII also reports the average energy partitioning among the reaction products. As expected, we find the rate coefficients to be much larger. However, the calculated energy partitioning is nearly identical to that previously obtained using the higher barrier potential surface.[8]

Figures 15 and 16 give RRK plots for reactions (R7) and (R8), respectively. For reaction (R7), the barrier height computed in paper I has been used for the critical energy. E_0 for reaction (R8) is taken to be the reaction endothermicity. s values are found to be 3.61 and 3.09 for reactions (R7) and (R8), respectively. The corresponding high-pressure limiting rates are $1.13\times10^{13}\exp[-1.513\,\text{eV}/RT]$ s^{-1} and $5.89\times10^{13}\exp[-3.28\,\text{eV}/RT]$ s^{-1}.

IV. SUMMARY

We have investigated the unimolecular decomposition dynamics of disilene using classical trajectories computed on a global potential-energy surface that has been fitted to the results of *ab initio* calculations and to experimental data for activation energies, heats of reaction, equilibrium structures, and measured fundamental vibrational frequencies. Metropolis sampling procedures were employed to average over the initial phase space of Si_2H_4.

We have found that extremely long Markov walks are required to sample a large percentage of the available Si_2H_4 phase space unless care is taken to optimize the walk param-

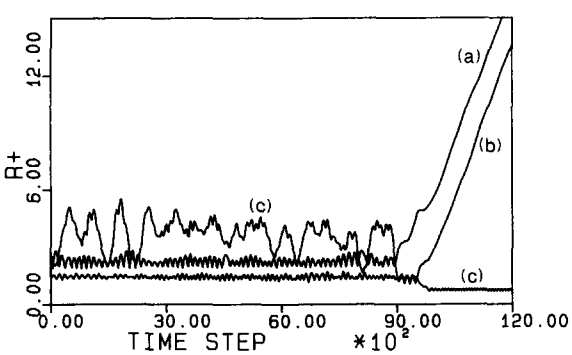

FIG. 12. Same as Fig. 9 but for a trajectory leading to reaction (R3). $R+$ represents (a) $R_2 + 0.75$ Å; (b) R_5; (c) R_{12}.

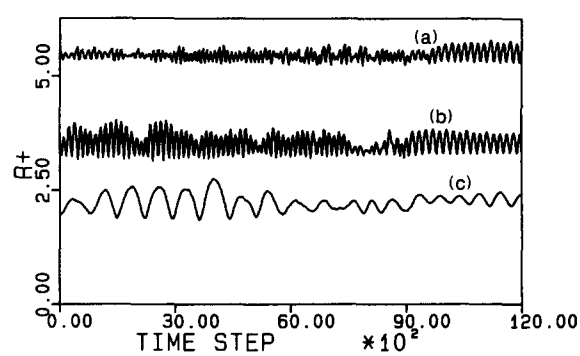

FIG. 14. Same as Fig. 12 but for (a) $R+ = R_4 + 4.0$ Å; (b) $R+ = R_3 + 2.0$; (c) $R+ = R_1$.

TABLE VII. Rate coefficients[a] and product energy distributions for the dissociation of SiH_2 as a function of internal energy. Notation is as defined in Table V and the text.

E (eV)	$k_7(E)$	$k_8(E)$	$\langle F_T \rangle$	$\langle F_R \rangle$	$\langle F_V \rangle$
3.0	1.79	0.0[b]	0.37	0.29	0.34
3.5	2.67	0.17	0.33	0.32	0.35
4.0	3.22	1.90	0.37	0.25	0.38
4.5	3.88	3.44	0.35	0.28	0.37

[a] Rate coefficients are given in units of $s^{-1} \times 10^{12}$.
[b] Zero entry means no trajectories were observed to dissociate into this channel at this energy.

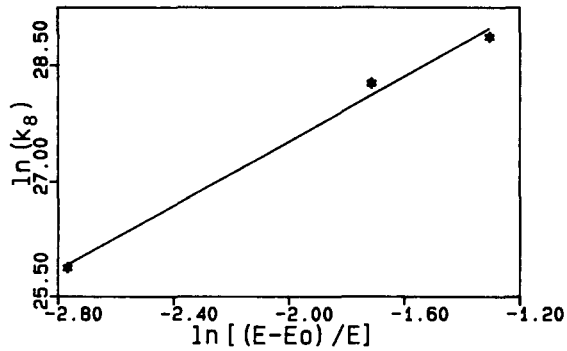

FIG. 16. Same as Fig. 5 for reaction (R8) with $E_0 = 3.28$ eV.

eters. This can be done most effectively by using different parameters for the different types of atoms present.

The most important Si_2H_4 dissociation channel is found to be the three-center elimination of molecular hydrogen leading to $H_2Si{=}Si$ as a product. At internal energies below 7.0 eV, the other decomposition channels are, in order of importance, Si–Si bond rupture to produce two SiH_2 molecules, four-center molecular hydrogen elimination leading to $HSi{=}SiH$, and simple Si–H bond rupture. At 8.0 eV and above, four-center H_2 elimination replaces Si–Si bond rupture as the second most important Si_2H_4 decomposition channel.

The microcanonical rate coefficients are well described by the RRK equation. The results suggest that five to nine of the Si_2H_4 vibrational modes are effectively coupled to the decomposition coordinate for Si–Si bond rupture and four-center molecular hydrogen elimination. An examination of the details of individual trajectories supports this conclusion in that the Si–H stretching modes are seen to be essentially unaffected by Si–Si bond rupture. The same is true for four-center molecular hydrogen elimination provided we refer to those Si–H bonds not directly involved in the dissociation process. The larger s value for three-center elimination is not completely understood.

The reaction mechanism for three-center dissociation is shown to involve a concerted breaking of both Si–H bonds followed immediately by the formation of H_2. In contrast, the four-center elimination channel involves a hydrogen atom transfer from one silicon atom to the other. This is then followed by the elimination of H_2 in a process that resembles a half-reaction of $H + Si_2H_3$.

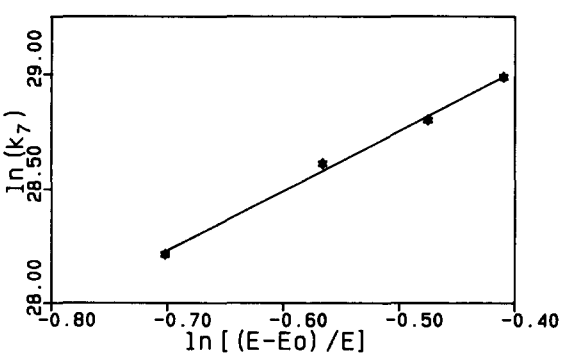

FIG. 15. Same as Fig. 5 for reaction (R7) with $E_0 = 1.513$ eV.

The energy partitioning among the dissociation products is nearly statistical. There is a propensity to partition some excess energy into rotation of the newly formed H_2 molecule. This is interpreted to mean that the reaction process frequently does not occur along a symmetric pathway but involves nonsymmetric structures which impart torque and angular momentum to the departing H_2 molecule. Most of the excess energy is found to reside in vibrational modes, which is in accord with the results of most MPD experiments on similar systems.

A study of the decomposition of Si_2H_4 complexes formed by the recombination of two SiH_2 molecules shows that the rates for both three- and four-center molecular hydrogen elimination are in agreement with those computed for Si_2H_4 molecules containing an equal amount of energy completely randomized among the available internal degrees of freedom present in the molecule. However, the rate of Si–Si bond rupture for such complexes is larger than that expected for systems in which the internal energy is fully randomized.

The decomposition dynamics of SiH_2 has been reexamined on the new global potential-energy surface. Due to the higher heat of formation of SiH_2 predicted by the most recent calculations,[3,5] the potential barriers for Si–H bond rupture and molecular hydrogen elimination are less than those predicted by the potential surface used in our previous studies.[8] As a result, we find that the decomposition rate coefficients are correspondingly larger. Energy partitioning among the products, however, is found to be virtually the same on the present potential surface as that computed in our previous work.[8]

ACKNOWLEDGMENTS

We are pleased to acknowledge financial support from the Air Force Office of Scientific Research under Grant No. AFOSR-86-0043. All calculations in this paper were carried out on a VAX 11/780 and a microVAX II purchased, in part, with funds provided by grants from the Department of Defense University Instrumentation Program, No. AFOSR-85-0115, and the Air Force Office of Scientific Research, No. AFOSR-86-0043. P.M.A. expresses his thanks to Vikram University, Ujjain, India, for granting him leave to pursue this research.

[1]P. M. Agrawal, D. L. Thompson, and L. M. Raff, J. Chem. Phys. **88**, 5948 (1988).
[2]J. Berkowitz, J. P. Greene, and H. Cho, J. Chem. Phys. **86**, 1235 (1987).
[3]P. Ho, M. E. Coltrin, J. S. Binkley, and C. F. Melius, J. Phys. Chem **89**, 4647 (1985); **90**, 3399 (1986).
[4]S. D. Peyerimhoff and R. J. Buenker, Chem. Phys. **72**, 111 (1982).
[5]M. S. Gordon, T. N. Truong, and E. K. Bonderson, J. Am. Chem. Soc. **108**, 1421 (1986).
[6]J. S. Binkley, J. Am. Chem. Soc. **106**, 603 (1984).
[7](a) M. E. Coltrin, R. J. Kee, and J. A. Miller, J. Electrochem. Soc. **131**, 425 (1984); (b) W. G. Breiland, M. E. Coltrin, and P. Ho, J. Appl. Phys. **59**, 3267 (1986).
[8]I. NoorBatcha, L. M. Raff, D. L. Thompson, and R. Viswanathan, J. Chem. Phys. **84**, 4341 (1986).
[9]R. Viswanathan, D. L. Thompson, and L. M. Raff, J. Phys. Chem. **89**, 1428 (1985).
[10]R. Walch, Acc. Chem. Res. **14**, 246 (1981).
[11]A. M. Doncaster and R. Walch, Int. J. Chem. Kinet. **13**, 503 (1981).
[12]L. M. Raff and D. L. Thompson, in *Theory of Chemical Reaction Dynamics, Vol. III*, edited by M. Baer (Chemical Rubber, Boca Raton, FL, 1985).
[13]L. M. Raff and R. W. Graham, J. Phys. Chem. (to be published).
[14]R. Viswanathan, D. L. Thompson, and L. M. Raff, J. Chem. Phys. **80**, 4230 (1984).
[15]J. W. Brady, J. D. Doll, and D. L. Thompson, J. Chem. Phys. **74**, 1026 (1981).
[16]J. P. Valleau and S. G. Whittington, in *Statistical Mechanics*, edited by B. J. Berne (Plenum, New York, 1977), p. 137.
[17]M. N. Saha and B. N. Srivastava, *A Treatise on Heat* (Indian Press, Allahabad, 1958), p. 186.
[18]B. E. Holmes and D. W. Setser, J. Phys. Chem. **79**, 1320 (1975); **82**, 2461 (1978).
[19]P. N. Clough, J. C. Polanyi, and R. T. Taguchi, Can. J. Chem. **48**, 2919 (1970).
[20]M. J. Berry and G. C. Pimentel, J. Chem. Phys. **49**, 5190 (1968).